Eur. Phys. J. D **13**, 323–328 (2001)

THE EUROPEAN PHYSICAL JOURNAL D

EDP Sciences

Electron impact single detachment on the F^- ions using the heavy ion storage ring CRYRING: Cross-section determination

K. Andersson[1], D. Hanstorp[1], A. Neau[2], S. Rosén[2], H.T. Schmidt[2], R. Thomas[2], M. Larsson[2], J. Semaniak[3], F. Österdahl[4], H. Danared[4], A. Källberg[4], and A. Le Padellec[5,a]

[1] Department of Physics, Chalmers University of Technology/Göteborg University, 412 96 Göteborg, Sweden
[2] Department of Physics, Stockholm University, Box 6730, 113 85 Stockholm, Sweden
[3] Institute of Physics, Pedagogical University, 25-405 Kielce, Poland
[4] Manne Siegbahn Laboratory, Frescativägen 24, 104 05 Stockholm, Sweden
[5] LCAR[b], Université Paul Sabatier-Toulouse III, 118 route de Narbonne, bâtiment III R1B4, 31062 Toulouse Cedex 4, France

Received 14 June 2000 and Received in final form 11 September 2000

Abstract. Electron Impact Single Detachment (EISD) of F^- has been studied using the heavy ion storage ring CRYRING at the Manne Siegbahn Laboratory, Stockholm, Sweden. F^- ions stored in the ring were merged with an electron beam in one of the ring sections. Neutral F atoms produced in the EISD process were detected in the zero-degree direction using a surface barrier detector. The threshold for the detachment process was found to be around 7.6 eV, thus more than twice the binding energy of F^-. The cross-sections increased smoothly up to 55 eV where it reached a maximum of 1.9×10^{-16} cm^2. At higher energies a slow decrease of the cross-section was observed, which follows the energy dependence predicted by the Bethe-Born approximation. The experiment showed that CRYRING can be used favourably for studies of anions, and several experiments are forthcoming.

PACS. 34.80.Dp Atomic excitation and ionization by electron impact – 32.10.Hq Ionization potentials, electron affinities

1 Introduction

In negative ions, the normally dominant Coulomb interaction between each electron and the ionic core is suppressed. The interelectronic interaction, and in particular, the so-called electron correlation effect, then becomes relatively more important. Under these conditions, the independent particle model, which adequately describes neutral and positively charged atomic systems, breaks down. Experimental studies of anions can therefore serve as a probe of the electron correlation effect, and hence be used to test theoretical models in order to get a better understanding of atomic and molecular processes. Most of the information on their structure has been obtained by studying the photodetachment process, in which the outermost electron is emitted due to the absorption of a photon. Branscomb carried out the pioneering experiments in the fifties, but it was in the seventies that Lineberger and coworkers performed the first systematic study [1]. By using neutral particle detection and electron spectroscopy, they managed to determine the ground state configuration of most atomic anions. More recently, the combination of photodetachment and resonance ionisation spectroscopy has been shown to be a powerful tool for the study of both bound and continuum states [2,3]. Electron impact studies on anions, on the other hand, were carried out by Tisone and Branscomb [4,5], Dance *et al.* [6] and by Peart *et al.* [7]. Later on, after the storage ring technology came into operation, a number of studies were performed by Andersen and collaborators [8,9], using ASTRID located at Aarhus University in Denmark. In this paper a study of electron impact detachment of F^- is presented.

Negative ions play important roles in many applications. Plasma properties are strongly dependent on whether the negative charges are in the form of highly mobile electrons or slowly moving anions. In order to correctly model a plasma, it is therefore important to know the energy dependent cross-sections for the various collisional processes, which involve anions. For plasma etching in the semiconductor industry, halogens are often used as active compounds [10,11], and a detailed knowledge of detachment and attachment rates for these systems are therefore of great importance. Detachment rates of halogens are also important in excimer laser technology. In such lasers, the lasing occurs in metastable excimer molecules, such as NeF, KrF or XeF. These molecules are

[a] e-mail: arnaud.lepadellec@irsamc.ups-tlse.fr
[b] UMR 5589

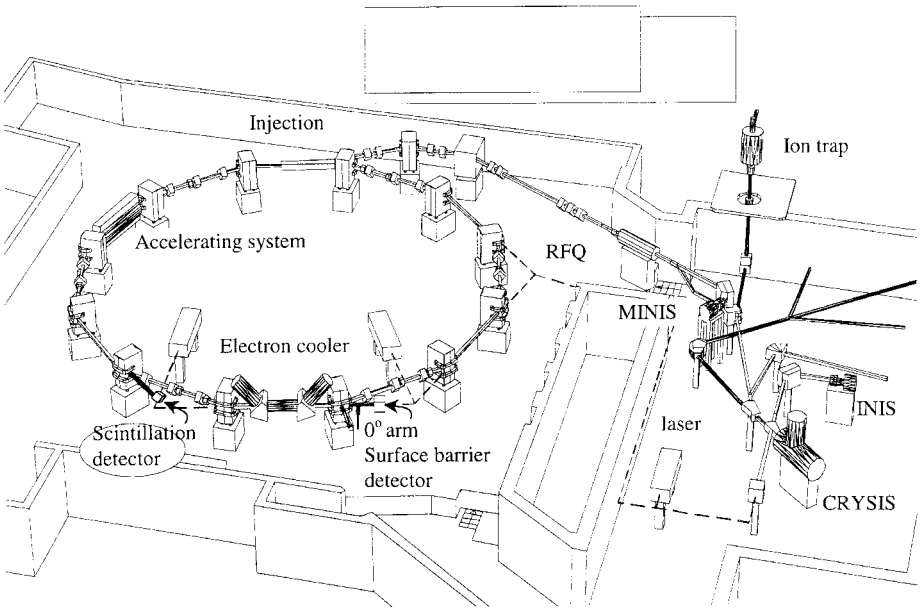

Fig. 1. The heavy ion storage ring CRYRING.

produced by the attachment of an isolated halogen atom to an excited noble gas atom, such as Ar, Kr or Xe. An isolated halogen atom in its negative charge state will not be able to associate to the noble gas atom, and it is consequently not able to participate in the lasing action. Therefore, such lasers could be made more efficient if a reaction scheme leading to a decreased anion production or an increased detachment rate, could be achieved. Modelling of such lasers hence requires accurate values of cross-sections for the production and destruction pathways of halogen anions [12].

In this paper we present the first study of negative ions performed at the CRYRING facility at the Manne Siegbahn Laboratory in Stockholm, where we have studied Electron Impact Single Detachment (EISD) on the F^- ion. The paper is organised as follows: the general features of the storage ring are introduced (Sect. 2) as well as the data analysis procedure to extract the cross-sections (Sect. 3). These cross-sections are then presented, discussed and put in perspective with those reported by others (Sect. 4), and a conclusion is given in Section 5.

2 Experiment

The experiment was performed at the heavy-ion storage ring CRYRING (see Fig. 1). This ring was mainly designed for storage of highly charged ions. Since the time the ring was put into operation in the beginning of the 1990's it has, however, also been shown to be a very powerful tool also for studies of singly charged molecular ions. With this experiment, we show that it can also be used to study electron-anion collisions. A brief description of the experimental facility will be given below. It is basically the same set-up as has been used for studies of electron impact of positive ions and detailed descriptions of the apparatus can be found elsewhere [13].

F^- ions were produced in a cesium sputter ion source [14]. In this source, positive cesium ions are accelerated towards a water-cooled solid cathode, from which cathode material will be sputtered. The choice of the cathode material is determined by the anion under production, and in this experiment a mixture of CaF_2 and silver powder was used. The cesium in the source will, in addition to being used for the sputtering, form a few monolayers on the cathode. Atoms and molecules sputtered from the target will, with a rather high probability, capture an electron while passing through the cesium layer and hence be emitted as negative ions. The ion current measured after a magnet used for mass analysis was typically a few microamperes. This type of source can be used to produce ion currents of the order of microamperes of most atomic and many molecular ions, simply by selecting the proper cathode material.

After extraction from the source at 40 keV, the F^- ions were injected into the ring and accelerated to the full energy of 5.05 MeV. The maximum beam energy is limited by the magnetic rigidity of the ring. The detachment lifetime for the ions, due to collisions with rest gas atoms and molecules, was 17 s at injection energy and 6 s at full energy. In the electron cooler section, the ion beam was merged with a collinear electron beam. These electrons have a velocity spread that can be described by an anisotropic Maxwell-Boltzmann distribution

$$f(v_e) = \frac{m_e}{2\pi k T_{e\perp}} \left(\frac{m_e}{2\pi k T_{e\parallel}}\right)^{1/2} \exp\left(-\frac{m_e v_{e\perp}^2}{2kT_{e\perp}} - \frac{m_e v_{e\parallel}^2}{2kT_{e\parallel}}\right), \quad (1)$$

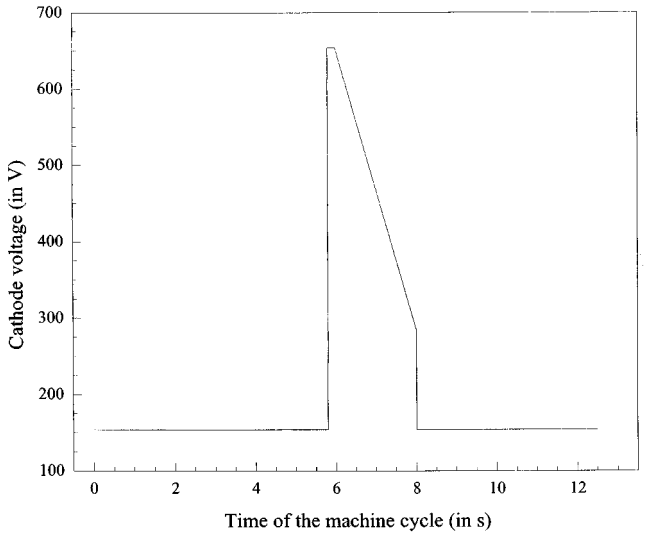

Fig. 2. The electron cooler cathode voltage as a function of time, as set for the scan between 20 and 173 eV in the centre-of-mass frame.

where $T_{e\parallel}$ and $T_{e\perp}$ represent the longitudinal and transverse temperatures, respectively, with $kT_{e\parallel} \approx 0.1$ meV and $kT_{e\perp} \approx 1$ meV.

Each experimental cycle, with a length of 12 s, consisted of five steps: injection, acceleration, cooling, measurement and dumping of the beam. One second was used for the injection and acceleration, and the cooling period was set to 4.8 s. During the latter time the ions interacted with velocity matched electrons. Collisions between the ions and the electrons caused a reduction in the thermal random motion of the ions, so called phase-space cooling. At this stage the collision energies were not sufficient to detach the extra electron from the F^- ion. When the ions had been cooled, the actual experiment started. This was achieved by detuning the electron velocity, creating a collision energy in the centre-of-mass-frame, E_{cm}, given by

$$E_{cm} = \left(\sqrt{E_e} - \sqrt{E_{cool}}\right)^2 . \quad (2)$$

E_e is the average electron energy in the laboratory frame and E_{cool} the cooling energy of the electrons. The latter energy is the energy of the electrons in the laboratory frame for which their velocity matches the velocity of the ions in the ring. For F^- at full energy, this is approximately 154 eV. In our experiment, collision energies between 0 and 173 eV were investigated in two independent scans. One long scan covered the energy range from 20 eV to 173 eV, and one with higher resolution was used to investigate the threshold region between 0 and 20 eV. Nevertheless, we restricted our data analysis to energies up to 130 eV in the centre-of-mass frame. The scan of the collision energy was achieved by changing the cathode voltage in the electron cooler. Figure 2 shows how the electron energy was changed during the long scan. After the cooling was completed, the cathode voltage was jumped by 500 V (thus 654 V in total), which gives an electron energy of 173 eV in the centre-of-mass frame. This voltage was kept for 0.2 s in order to allow the electron beam to stabilize. During the next two seconds, the cathode voltage was ramped down by 369 V to reach the lowest cathode voltage of 285 V, thus giving a final centre-of-mass energy of 20 eV. The cathode voltage was then, within 2 ms, scanned up to the cooling energy again, before the ion beam was finally dumped and all settings of the ring was returned to the values for a new injection.

The fast fluorine atoms coming from the EISD process and from background gas collisions, were unaffected by the ring magnetic field. They followed their original trajectory and impinged on a energy-sensitive surface barrier detector (SBD), which was placed in the so-called zero-degree arm, 3.5 meters downstream from the interaction region. The signal from the detector was amplified and analyzed using a discriminator circuit. Signals accepted by the discriminator were then fed into a multichannel scaler (MCS) that was triggered at the start of each new injection into the ring. The MCS records the number of pulses *versus* time. Thus, by a simple time to energy correlation, the signal *versus* the centre-of-mass energy is obtained. The destruction of the ion beam due to collisions with the rest gas was monitored separately with a scintillation detector placed in another section of the ring. This signal was then recorded with another MCS.

3 Data analysis

An experimental problem arose from the fact that the signal from the surface barrier detector (SBD) saturated at rather small beam currents, whereas the current measurements, performed with a current transformer, required an intense beam. As will be described in detail below, this problem was solved by relating each of the signals, recorded at different beam currents, to the signal from the scintillator detector, a device with a very high dynamical range.

The experimental Electron Impact Single Detachment (EISD) rate coefficient $\langle v_d \sigma \rangle$ for a given centre-of-mass energy is given by [15,16]

$$\langle v_d \sigma \rangle = R_B \frac{C}{n_e l} \frac{N_{EISD}}{C_{Scint}} . \quad (3)$$

In this expression, C is the circumference of the ring, l the length of the electron cooler and n_e the electron density. N_{EISD} represents the number of counts from the E_{ISD} process at a given centre- of-mass energy. This value is obtained by subtracting the number of counts when the collision energy was set to E_{cool} from the value obtain when the collision energy was set to E_{cm}.

Simultaneously, another independent MCS spectrum, labelled C_{Scint}, was recorded with the scintillation detector. The last parameter in equation (3), R_B, is the destruction rate per ion and per time unit, and can be derived from another MCS spectrum taken with the same scintillation detector, but acquired at the same time as the ion

current measurement I_i. This is given by

$$R_\mathrm{B} = \frac{\mathrm{d}C_\mathrm{Scint}}{\mathrm{d}t}\frac{1}{I_\mathrm{i}}fe, \tag{4}$$

where f represents the revolution frequency of the ions (the so-called Schottky frequency) and e the elementary charge. Typical values for the ion current at injection time, the electron current (constant at any time) and the electron density at cooling energy were 350 nA, 3.56 mA and 2×10^7 cm^{-3}, respectively. The measured rate coefficient $\langle v_\mathrm{d}\sigma\rangle$ is then related to the cross-section by

$$\langle v_\mathrm{d}\sigma\rangle = \int f(v_\mathrm{d}, v)\sigma(v)v\,\mathrm{d}^3v, \tag{5}$$

where $f(v_\mathrm{d}, v)$ is the electron velocity distribution (see Eq. (1)) around the averaged centre-of-mass velocity v_d.

Two corrections [13] have to be performed. First, the centre-of-mass energy had to be corrected for the space charge of the electron beam. Second, due to the geometry of the electron cooler, the ions did not only interact with electrons on a straight section, but also in the curved regions where the relative velocity is different. As a result, the number of counts, recorded by the detector at a given energy, also came from reactions that occur at somewhat larger centre-of-mass energies, resulting in a distortion of the true signal. An iterative procedure was used for this correction, as described by Lampert *et al.* [17]. This was essential in order to define the correct threshold for the EISD process found at 7.6 eV whereas the uncorrected one appeared at the somewhat lower energy of 6 eV. Moreover, the cross-sections at their maximum were shifted downwards by about a factor of three after that toroidal correction.

4 Results and discussion

Figure 3a in full squares represents our new measurement of the cross-section for the Electron Impact Single Detachment of F^- from threshold up to 130 eV, *i.e.* the process

$$F^-(1s^2 2s^2 2p^6\ {}^1S_0) + e^- \rightarrow F(1s^2 2s^2 2p^5\ {}^2P_{3/2}) + 2e^-.$$

The horizontal axis shows the centre-of-mass energy with an energy resolution ranging from 80 meV at 7.6 eV (threshold location) to 325 meV at the maximal investigated energy of 130 eV, and the error bars along the vertical axis represent only the statistical uncertainties on our cross-sections. These are given by $\sqrt{S+2B}/S$ since we extract our signal S from a rest gas collision induced background B, by the straightforward subtraction $(S+B)-B$. The graph does not include the 16% systematic uncertainties, that we estimate to be at a one sigma level, in order to show the overall shape of our measured cross-sections. These systematic uncertainties are divided as follows: 10% on the ion current measurement, 1% on the circumference of the ring, 10% on the length of the interaction region, 2% on the electron current, 7% on the electron current distribution, every contribution being added quadratically. The straightness of the magnetic field defines the length of the interaction region. The uncertainty on the field measurements to define that region was found to be 10%; consequently, we believe that the same value shall be considered on the length of the interaction region. The 7% uncertainty on the electron current distribution comes from a computation of the electron trajectories within the gun. Therefore, our whole cross-section curve in Figure 3a could be shifted up or down by 16%, within the uncertainty. That curve displays the typical trend for such a detachment process: the cross-section rises from zero at the threshold E_th to a maximum value and then decreases monotonically as $(1/E)\ln(E)$, according to the Bethe-Born formalism [18]. The location of the threshold and the magnitude on top of the cross-sections bring some interesting insights to the detachment mechanism. For comparison, the results reported by Peart *et al.* [19] are shown as open squares, and once again, only the statistical uncertainties are displayed. One would have to account for an extra 7% to include their systematic errors. The overall shape of the cross-section curves is similar, but ours is about 30% lower; this is not serious disagreement however, since both sets of data match within the total uncertainties (statistical plus systematic).

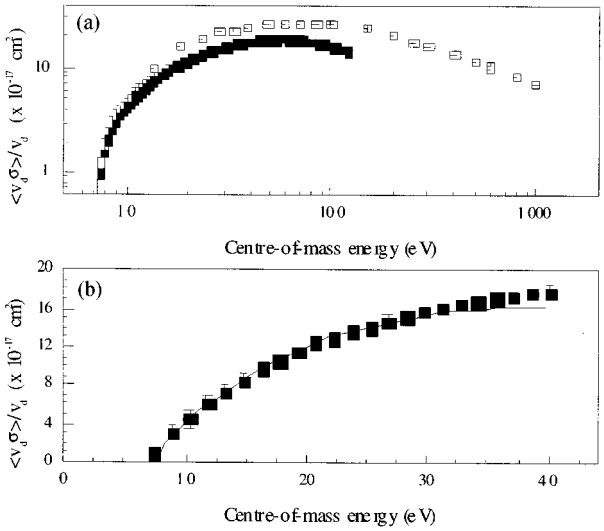

Fig. 3. (a) Our absolute EISD cross-sections $\langle v_\mathrm{d}\sigma\rangle/v_\mathrm{d}$ from threshold up to 130 eV (in full squares and with statistical error bars only – see text) together with those by Peart *et al.* [19] (in open squares with the same type of error bars). (b) The same cross-sections around threshold in full squares as they compare in full line to the classical model by Andersen *et al.* [8,20].

A simple classical model, in which it is assumed that the incoming electron experiences a purely repulsive Coulomb potential, has been developed and used by Andersen *et al.* [8,20]. This model has previously been used to correctly predict the cross-section behaviour near the threshold, despite the fact that detachment through tunneling is neglected. This model is shown in full line in Figure 3b together with our near threshold data in full squares.

Near the threshold the cross-section, as a function of the energy of the projectile E, can be expressed as

$$\sigma = p\pi R^2 \left(1 - \frac{E_{\rm th}}{E}\right), \tag{6}$$

where p is a scaling factor which describes the probability for the detachment process to occur within a certain reaction radius R. This parameter R is directly related to the threshold $E_{\rm th}$, as well as to the spatial extension of the valence electrons a, according to the formula

$$R = \frac{1}{E_{\rm th}} = \left(\frac{E_{\rm B}}{a}\right)^{-1/2} \tag{7}$$

where the R and a parameters on one hand, the $E_{\rm th}$ and $E_{\rm B}$ energies on another hand, have to be expressed in atomic units, namely in Bohrs and Hartrees, respectively. When we fitted equation (6) to our near threshold cross-sections, we obtained a scaling probability $p = 0.70$ and a reaction radius $R = 3.6a_0$. Consequently, the apparent threshold and spatial extension a are found to be $E_{\rm th} = 0.28$ Hartree $= 7.6$ eV and $1.6a_0$, respectively. This latter parameter is consistent with the classical radius of the F^- anion of $2.2a_0$. We are aware that the statistical uncertainties are larger around the threshold due to the low count rate, but we are confident within less than 2% with the parameters extracted from the model used above.

Secondly, we investigated the magnitude of the EISD cross-sections at the peak of the cross-section using a relation derived by Smirnov (1968) for electron impact cross-sections, in the framework of Thomson's classical theory [21]. This formula is used to relate the magnitude of the EISD cross-sections of two atomic anions $\sigma_{\rm A1}$ and $\sigma_{\rm A2}$, and this is expected to yield results within an order of magnitude of the correct value. With $E_{\rm B\ A1,A2}$ and $n_{\rm A1,A2}$ being the binding energies and the effective numbers of active electrons in the outer shells of the two anions, this formula can be expressed as

$$\frac{\sigma_{\rm A1}}{\sigma_{\rm A2}} = \frac{n_{\rm A1}}{n_{\rm A2}} \left(\frac{E_{\rm B\ A2}}{E_{\rm B\ A_1}}\right)^2. \tag{8}$$

This tells us that the largest binding energy of the anion, and hence the smallest spatial extension a, will give the smallest EISD cross-section. We now use equation (8) to estimate the maximum EISD for F^-. Andersen *et al.* [20,22] have measured the absolute cross-sections for D^-, which gave a maximum value of 3×10^{-15} cm^2. Using equation (8) to relate the cross-section of D^- ($n_{D^-} = 2$) and F^-, we obtain a ratio of 0.14, if we assume that only the six $2p$-electrons are active in F^-. The Thomson's formula then gives a maximum cross-sections for F^- of about 4.3×10^{-16} cm^2, which is a bit more than twice our experimental result.

A careful study of our experimental data does not reveal any structure apart from the major trends, *i.e.* an increase up to 55 eV followed by a slow decrease at higher energies. The lack of structure is interesting from two points of view.

First, this means that we cannot see any indication of the prediction by Ormonde [23], who found from his calculations that long-lived ^{1}D and ^{1}P shape resonances lying above $F(2p^5\ ^2P_{3/2})$ could give rise to near-threshold cross-sections as large as $2{-}3 \times 10^{-15}$ cm^2. We cannot exclude the existence of such resonance with a width of only 2 meV, since our experimental resolution was about 80 meV around threshold. Such very narrow resonance could have been hidden in the noise. Moreover, there is another resonance which might have been observed in the energy range under study and which could have resulted from the $2p^4(^1D)3s^2\ ^1D$ doubly excited state located 14.85 eV above the $2p^6\ ^1S_0$ ground state of the anion [24]. We do not see any evidence for it, and the reason shall be the same than for the shape resonances discussed above, namely the lack of energy resolution.

Second, short-lived atomic dianions would reveal themselves as structures in the EIDS cross-sections. Walton, Peart and Dolder claimed observations of such resonances in earlier measurements on H^- [25–27] and O^- [28], although nobody else has reported similar observations since. It is important to point out that the situation in F^- is somewhat different from H^- or O^-. The F anion is a closed p-shell ($2p^6$) whereas H^- and O^- are a closed s-shell ($2s^2$) and an open p-shell ($2p^5$), respectively. One would be tempted to believe that it is more difficult to attach an extra electron when the target anion has a noble gas structure. The question of doubly charge negative ions is, however, not closed since Bylicki and Nicolaides [29] and independently Sommerfeld *et al.* [30] have recently performed calculations which claim the evidence for a resonance state of H^{2-}, whereas Robicheaux claimed the opposite [31].

We will finally attempt to discuss how the EISD process might occur in a strongly bound anion such as F^-, for which a low dipole polarisability α results from the large binding energy. Indeed, for the F^- anion, α is equal to 14.5 au [32], as compared with 430.5 au for B^-. In the "sudden" approximation that was demonstrated to be valid for B^-, the "shake-off" parameter S gives the detachment probability as

$$S = \left(\frac{I_{\rm DD}}{I_{\rm SD}}\right)\left(\frac{\sigma_{\rm DD}}{\sigma_{\rm SD}}\right), \tag{9}$$

where $I_{\rm DD,SD}$ (here 20.8 eV and 3.4 eV) and $\sigma_{\rm DD,SD}$ represent the ionisation potentials and maximum cross-sections for the double and single detachment, respectively. The cross-sections for the Electron Impact Double Detachment on F^- are taken from the work by Steidl [33], and combined with those of the present work. Using equation (9), one would find for the shake off parameter of F^-, a value of 90% that is in the same order than that was found for B^- by Andersen *et al.* [34]. This is surprising, bearing in mind the large difference in their electron affinities and dipole polarisabilities. This could mean that the "sudden approximation" is not valid for F^-.

5 Conclusion

In this paper we have presented the first experiment on negative ions using the heavy ion storage ring CRYRING at the Manne Siegbahn Laboratory in Stockholm, Sweden. Our results on Electron Impact Single Detachment (EISD) on F^- shows that CRYRING can be used favourably for studies of these ions. In our experiment, the photodetachment threshold was found at around 7.6 eV, more than twice the electron affinity of F. This is a common feature to all of the atomic anions studied so far. The cross-section increases monotonically up to a value of 1.9×10^{-16} cm^2, which is about half the value given by the Thomson's scaling model, and then decreases with increasing energy, according to the Bethe-Born formalism. Our data agree within the uncertainties with the previous experimental work by Peart *et al.* [19] who used a crossed beam set-up. The positive results of this work will be continued with studies of several atomic as well as molecular negative ions.

This work was supported by the Swedish National Science Research Council (NFR) and by the Manne Siegbahn Laboratory through their program for new external users. We thank the staff of the Manne Siegbahn Laboratory for their invaluable help and use of the heavy ion storage ring facility.

References

1. H. Hotop, W.C. Lineberger, J. Phys. Chem. Ref. Data **14**, 731 (1985).
2. V.V. Petrunin, J.D. Voldstad, P. Balling, P. Kristensen, T. Andersen, H.K. Haugen, Phys. Rev. Lett. **75**, 1911 (1995).
3. G. Haeffler, D. Hanstorp, I. Kiyan, A.E. Klinkmüller, U. Ljungblad, D.J. Pegg, Phys. Rev. A **53**, 4127 (1996).
4. G. Tisone, L.M. Branscomb, Phys. Rev. Lett. **17**, 236 (1966).
5. G. Tisone, L.M. Branscomb, Phys. Rev. **170**, 169 (1968).
6. D.F. Dance, M.F.A. Harrison, R.D. Rundel, Proc. R. Soc. Lond. A **299**, 525 (1967).
7. B. Peart, D.S. Walton, K.T. Dolder, J. Phys. B **3**, 1346 (1970).
8. L. Vejby-Christensen, D. Kella, D. Mathur, H.B. Pedersen, H.T. Schmidt, L.H. Andersen, Phys. Rev. A **53**, 2371 (1996).
9. L.H. Andersen, T. Andersen, P. Hvelplund, Adv. At. Mol. Opt. Phys. **38**, 155 (1997).
10. J.K. Olthoff, Y. Wang, J. Vac. Sci. Tech. A **17**, 1552 (1999).
11. L.G. Christophorou, J.K. Olthoff, J. Phys. Chem. Ref. Data **28**, 131 (1999).
12. J. Hsia, Appl. Phys. Lett. **30**, 101 (1977).
13. C. Stromholm, J. Semaniak, S. Rosen, H. Danared, S. Datz, W. van der Zande, M. Larsson, Phys. Rev. A **54**, 3086 (1996).
14. Peabody Scientific, Peabody, Massachusetts - USA.
15. S. Rosén, A.M. Derkatch, J. Semaniak, A. Neau, A. Al-Khalili, A. Le Padellec, L. Vikor, H. Danared, M. af Ugglas, R. Thomas, M. Larsson, Faraday Discuss. **115**, 295 (2000).
16. A. Neau, A. Al-Khalili, S. Rosén, J. Semaniak, A. Le Padellec, A.M. Derkatch, W. Shi, L. Vikor, M. Larsson, R. Thomas, M. Nagard, K. Andersson, H. Danared, M. af Ugglas, J. Chem. Phys. **113**, 1762, (2000).
17. A. Lampert, A. Wolf, D. Habs, J. Kettner, G. Kilgus, D. Schwalm, M.S. Pindzola, N.R. Badnell, Phys. Rev. A **53**, 1413 (1996).
18. M. Inokuti, Y.-K. Kim, Phys. Rev. Lett. **173**, 154 (1968).
19. B. Peart, R. Forrest, K.T. Dolder, J. Phys. B **12**, L115 (1979).
20. L.H. Andersen, D. Mathur, H.T. Schmidt, L. Vejby-Christensen, Phys. Rev. Lett. **74**, 892 (1995).
21. B.M. Smirnov, *Atomic Collisions and Elementary Processes in Plasma* (Atomizdat, Moscw, 1968).
22. L.H. Andersen, D. Mathur, H.T. Schmidt, L. Vejby-Christensen, Phys. Rev. Lett. **74**, 1616 (1995).
23. S. Ormonde, Phys. Rev. Lett. **38**, 690 (1977).
24. J. Poulsen, T. Andersen, R.D. Cowan, P. Dahl, J.E. Hansen, J. Engholm Pedersen, J. Phys. B **23**, 457 (1990).
25. D.S. Walton, B. Peart, K.T. Dolder, J. Phys. B **3**, L148 (1970).
26. D.S. Walton, B. Peart, K.T. Dolder, J. Phys. B **4**, 1343 (1970).
27. B. Peart, K.T. Dolder, J. Phys. B **6**, 1497 (1973).
28. B. Peart, R.A. Forrest, K.T. Dolder, J. Phys. B **12**, 2735 (1979).
29. M. Bylicki, C.A. Nicolaides, J. Phys. B **31**, L685 (1998).
30. T. Sommerfeld, U.V. Riss, H.-D. Meyer, L.S. Cederbaum, Phys. Rev. A **55**, 1903 (1997).
31. F. Robicheaux, R.P. Wood, C.H. Green, Phys. Rev. A **49**, 1866 (1994).
32. R. Medeiros, M.A. Castro, O.A.V. Amaral, Phys. Rev. A **54**, 3661 (1996).
33. M. Steidl, Diplomarbeit, Giessen University, 1994.
34. L.H. Andersen, M.J. Jensen, H.B. Pedersen, L. Vejby-Christensen, N. Djuric, Phys. Rev. A **58**, 2819 (1998).